

Band gap changes of GaN shocked to 13 GPa

M. D. McCluskey^{a)} and Y. M. Gupta

Institute for Shock Physics and Department of Physics, Washington State University, Pullman, Washington 99164-2816

C. G. Van de Walle, D. P. Bour, M. Kneissl, and N. M. Johnson

Xerox PARC, 3333 Coyote Hill Rd., Palo Alto, California 94304

(Received 24 October 2001; accepted for publication 19 December 2001)

The band gap of GaN under uniaxial-strain compression was determined using time-resolved optical transmission measurements in shock-wave experiments. Shock waves were generated by impacting the GaN samples with *c*-cut sapphire impactors mounted on projectiles fired by a gas gun. Impact velocities were varied to provide longitudinal stresses ranging from 4.5 to 13 GPa. An abrupt increase of the band gap is observed upon shock-wave compression, followed by a slower increase. By measuring the absorption threshold before and during shock compression of the GaN layer, the band-gap shift for a particular longitudinal stress was obtained. A linear fit to the data yields a band-gap shift of 0.02 eV/GPa. Comparison with *ab initio* calculations show that this slope lies between the calculated bounds for isotropic and uniaxial compression. Potential reasons for the differences are indicated. © 2002 American Institute of Physics. [DOI: 10.1063/1.1455148]

GaN and related alloys, InGaN and AlGaN, have generated considerable interest for wide-band-gap devices such as blue laser diodes¹ and high-temperature, high-power transistors.² Since the different materials in device heterostructures have large lattice mismatches, strain effects are important. In InGaN alloys grown on GaN, for example, pseudomorphic strain has a significant effect on measured values of the band gap.³ To investigate how strain influences the optical properties of GaN, the effect of biaxial strain^{4,5} and hydrostatic pressure^{6,7} have been investigated in previous studies. Shock-wave experiments are well suited for examining strain effects in crystals because *uniaxial* strain is produced. In the present work, the band gap of GaN under uniaxial-strain compression was determined. An advantage of uniaxial strain is its simplicity: in the elastic limit, only the *c*-lattice constant is compressed, while the *a*-lattice constant remains unchanged. Through comparison with *ab initio* calculations, the results of these experiments provide insight into the optical properties of strained GaN.

GaN samples used in this study were grown by metalorganic chemical vapor deposition to a thickness of 4 μm on a *c*-cut sapphire substrate that was polished on both sides. For the impact experiments, the GaN layer was backed by a *c*-cut sapphire buffer. Shock waves were generated by impacting the sapphire substrate with a *c*-cut sapphire impactor mounted on a projectile fired by a light gas gun.⁸ The shock wave traveled through the sapphire substrate, the GaN epilayer, and the sapphire buffer. Longitudinal stresses were determined from the known shock response of *c*-cut sapphire.⁹ Impact velocities were varied from 0.20 to 0.55 km/s to provide stresses ranging from 4.5 to 13 GPa. The sample was at room temperature during the measurements. A Xenon flashlamp provided the incident UV and visible light. Transmitted light was dispersed using a spectrometer and recorded using a streak camera/charge coupled device detection sys-

tem. A shorting pin was placed near the sample to provide a trigger pulse. Time-resolved optical absorption measurements, similar to those described in Refs. 10 and 11, were carried out.

The light intensity as a function of wavelength was recorded in 20-ns intervals, or tracks. Prior to each impact experiment, a reference streak was recorded for a *c*-cut sapphire sample. The arrival of the shock wave at the GaN epilayer causes an abrupt change in the transmitted light. The absorbance values were obtained by the expression

$$\text{Absorbance} = \log_{10}(I_R/I), \quad (1)$$

where I_R and I are the transmitted light intensities through the sapphire reference and GaN samples, respectively. Figure 1 shows the absorbance versus photon energy for a GaN sample ~ 40 ns prior to [Fig. 1(a)] and ~ 40 ns after [Fig. 1(b)] the arrival of the shock wave with a stress of 4.5 GPa. Absorbance plots are also shown for GaN shocked at stresses

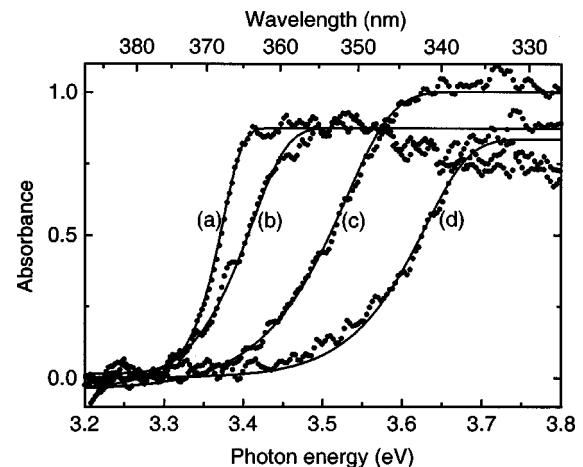


FIG. 1. Absorbance versus photon energy for a GaN sample that is (a) unshocked, and (b) shocked to a stress of 4.5 GPa. Absorbance plots are also shown for GaN shocked to stresses of (c) 9.2 GPa and (d) 12.6 GPa.

^{a)}Electronic mail: mattmcc@wsu.edu

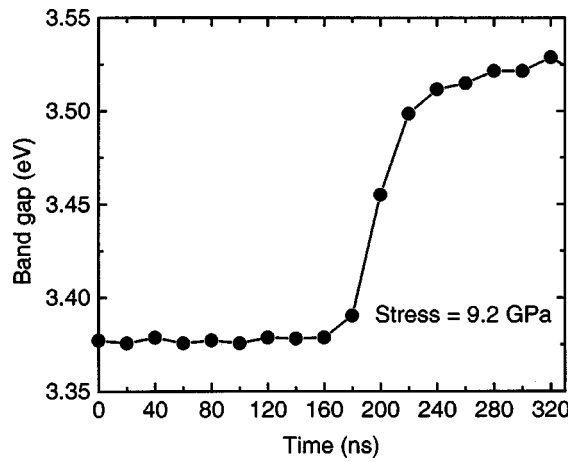


FIG. 2. Time dependence of the band-gap change of GaN shocked to 9.2 GPa.

of 9.2 GPa [Fig. 1(c)] and 12.6 GPa [Fig. 1(d)], each at ~ 40 ns after the arrival of the shock wave. As shown in Fig. 1, shocked GaN exhibits a blueshift and broadening of the band-gap absorption profile.

The time dependence of the band-gap change is shown in Fig. 2. In this plot, the band gap is taken to be the energy at which the absorbance is 0.5. An abrupt increase in the band gap is observed at a time $t=200$ ns. Since the signal is integrated over 20 ns, both the shocked and unshocked states are measured during the $t=200$ ns track, leading to a time-averaged value for the band gap. After the rapid increase, the band gap increases at a slower rate ($0.3 \text{ eV}/\mu\text{s}$). The rapid and subsequent “slow” increase in the band gap was observed in all the experiments. For consistency, the shocked band gap was taken to be the band gap two tracks (40 ns) after the first abrupt increase.

The solid lines in Fig. 1 are fits to the data, as explained next. The absorption threshold of unshocked GaN was modeled with a complementary error function:

$$\alpha_u(E) = (\alpha_0/2) \operatorname{erfc}[(E - E_0)/\Delta E_0], \quad (2)$$

where α_u is the absorption coefficient, E is the photon energy, and $\alpha_0 = 1.3 \times 10^5 \text{ cm}^{-1}$ (Ref. 12). The shocked-GaN absorption profile is described by the expression

$$\alpha_s^{(0)}(E) = \alpha_u(E - \delta E), \quad (3)$$

where δE is the shift in the absence of broadening. To account for broadening, Eq. (3) is convolved with an Airy function (Ai):

$$\alpha_s(E) = \int_{-\infty}^{\infty} \alpha_s^{(0)}(E') Ai \left[\frac{E' - E}{\Delta E_1} \right] \frac{dE'}{\Delta E_1}. \quad (4)$$

The parameters E_0 , ΔE_0 , δE , and ΔE_1 were adjusted to fit the data. In all the experiments, the absorption profiles are well modeled by values of $E_0 = 3.54 \pm 0.04 \text{ eV}$, $\Delta E_0 = 0.11 \pm 0.02 \text{ eV}$, and $\Delta E_1 = 0.10 \pm 0.02 \text{ eV}$.

Equation (4) is most often used to model the broadening of the band-gap absorption threshold due to the presence of electric fields (Franz-Keldysh effect).¹³ This broadening leads to a decrease in the absorption threshold energy by approximately ΔE_1 . The presence of large electric fields in shocked GaN would be consistent with the piezoelectric

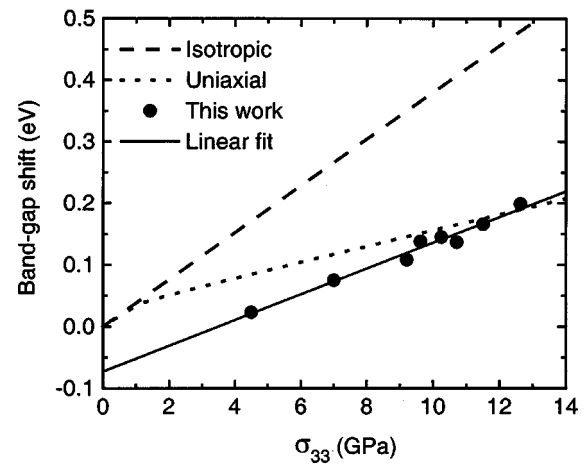


FIG. 3. Theoretical band-gap shift versus longitudinal stress (σ_{33}) for isotropic compression (dashed line) and uniaxial compression (dotted line). A linear fit to the experimental data is shown by the solid line. The negative intercept value is an artifact due to the broadening of the absorption threshold.

effect.¹⁴ However, other factors such as stress inhomogeneity and the formation of defects may also contribute to a broadening of the band-gap absorption threshold.

A background signal in the detection system led to a saturation of the absorbance (Fig. 1). To account for this experimental artifact, the absorbance was modeled by the expression

$$\text{Absorbance} = \log_{10} \left(\frac{I_0 + I_B}{I_0 \exp(-ad) + I_B} \right), \quad (5)$$

where $d = 4 \mu\text{m}$ is the GaN thickness, I_0 is the light intensity through the sapphire reference sample, and I_B is the background signal. The solid lines in Fig. 1 are fits to the data, using Eqs. (2)–(5).

To provide a consistent measure of the band-gap shift due to shock compression, the band gap was taken to be the energy at which $ad = 1.15$; in the absence of a background signal, this value corresponds to an absorbance of 0.5. The band-gap shift is plotted as a function of longitudinal stress in Fig. 3. A linear least-squares fit to the data yields

$$\Delta E_G = (-0.07 \pm 0.02) + (0.021 \pm 0.002) \sigma_{33}, \quad (6)$$

where ΔE_G is the band-gap shift (eV) and σ_{33} is the stress along the c axis (GPa). Compressive stresses and strains are defined as positive. The negative value of the intercept in Fig. 2 is due to the broadening of the absorption threshold discussed previously.

Ab initio calculations were performed for two bounding cases: isotropic and uniaxial compression. The calculations were based on density functional theory and *ab initio* pseudopotentials, using the nonlinear core correction.^{15,16} For isotropic compression, previous calculations¹⁶ yielded a band-gap shift of

$$\Delta E_G = 8.0 \Delta V/V, \quad (7)$$

where $\Delta V/V$ is the fractional volume change.

For purely uniaxial compression, only $\epsilon_{33} \neq 0$ (ϵ_{11} and ϵ_{33} are the strains along the a and c axes, respectively). The “A” and “B” band gap shifts are then given by^{17,18}

$$\Delta E_A = (D'_1 + D_3) \epsilon_{33} \quad (8)$$

$$\Delta E_B = [\Delta_1 + 3\Delta_2 + (2D'_1 + D_3) \epsilon_{33}] / 2 - \sqrt{(\Delta_1 - \Delta_2 - D_3 \epsilon_{33})^2 / 4 + 2\Delta_2^2} \quad (9)$$

where $D'_1 = D_1 - a_c$ is the deformation potential referenced to the conduction band minimum. The band-gap shifts given by Eqs. (8) and (9) were fitted to the *ab initio* calculations. Since the calculations neglected spin-orbit splitting, Δ_2 was set to zero during the fitting. A least-squares fit yielded values of $D'_1 = 5.14$ eV and $D_3 = 8.12$ eV.

For purely uniaxial deformation, the strain ϵ_{33} is related to the longitudinal stress by $\epsilon_{33} = \sigma_{33} / C_{33}$, where $C_{33} = 398$ GPa (Ref. 19); the contracted notation is used for the elastic constants. For isotropic deformation, the volume change is related to the stress by $\Delta V / V = 3\sigma_{33} / (2C_{13} + C_{33})$, where $C_{13} = 106$ GPa (Ref. 19). Equations (7)–(9) can then be expressed in terms of σ_{33} and compared with the experimental results, for which σ_{33} is known. It should be noted that for a given value of σ_{33} , the values of σ_{11} and σ_{22} depend on the nature of the deformation, and are different for isotropic and uniaxial compression. The calculated band-gap shifts for isotropic and uniaxial deformations are plotted in Fig. 3. In the case of uniaxial deformation, the discontinuity in the slope of the calculated band gap is due to a crossing of the valence bands. The band-gap minimum is plotted for values of $\Delta_1 = 22$ meV and $\Delta_2 = 5$ meV (Ref. 18).

We note that the slope of the experimental curve is *larger* than that of the calculated curve for uniaxial compression. This finding raises two possibilities: the calculated deformation potentials are not entirely accurate, or the GaN unit cell undergoes nonuniaxial deformation. The latter response is expected when plane shock wave compression of crystals results in elastic-plastic deformation.²⁰ Whether shocked GaN is undergoing elastic-plastic deformation at the stresses considered in the present work will require an independent determination of its mechanical response in plate-impact experiments. After the initial shock, the slow increase in the band gap (Fig. 3) is consistent with a gradual deformation toward nonuniaxial compression at the lattice level. An alternate explanation is that time-dependent screening of piezoelectric fields results in the slow band-gap increase.

In conclusion, the band gap of GaN under uniaxial compression has been determined using time-resolved optical

transmission measurements in shock-wave experiments. An important feature of the present work is that the samples are subjected to the macroscopically exact condition of uniaxial strain. An abrupt increase of the band gap is observed upon compression, followed by a slower increase. In the future, to resolve the apparent contradiction between experiment and theory, continuum measurements will be performed to determine the mechanical response of GaN to shock compression.

The authors are pleased to acknowledge A. Royalty, S. Thompson, and K. Zimmerman for assistance with target preparation and impact experiments. P. Rigg and L. Romano are thanked for numerous helpful discussions. The work at Washington State University was supported by the DOE Grant DE-FG03-97SF21388. The work at Xerox was supported by DARPA/MDA972-96-3-0014.

¹S. Nakamura, Mater. Res. Soc. Symp. Proc. **482**, 1145 (1998).

²*Wide-Band-Gap Semiconductors for High Power, High Frequency, and High Temperature*, edited by S. Denbaars, M. S. Shur, J. Palmour, and M. Spencer (Materials Research Society, Pittsburgh, 1998), Vol. 512.

³M. D. McCluskey, C. G. Van de Walle, C. P. Master, L. T. Romano, and N. M. Johnson, Appl. Phys. Lett. **72**, 2725 (1998); C. Wetzel, T. Takeuchi, S. Yamaguchi, H. Katoh, H. Amano, and I. Akasaki, *ibid.* **73**, 1994 (1998).

⁴W. Shan, R. J. Hauenstein, A. J. Fischer, J. J. Song, W. G. Perry, M. D. Bremser, R. F. Davis, and B. Goldenberg, Phys. Rev. B **54**, 13460 (1996).

⁵S. Chichibu, A. Shikanai, T. Azuhata, T. Sota, A. Kuramata, K. Horino, and S. Nakamura, Appl. Phys. Lett. **68**, 3766 (1996).

⁶W. Shan, T. J. Schmidt, R. J. Hauenstein, J. J. Song, and B. Goldenberg, Appl. Phys. Lett. **66**, 3492 (1995).

⁷P. Perlin, L. Mattos, N. A. Shapiro, J. Kruger, W. S. Wong, T. Sands, N. W. Cheung, and E. R. Weber, J. Appl. Phys. **85**, 2385 (1999).

⁸G. R. Fowles, G. E. Duvall, J. Asay, P. Bellamy, F. Feistmann, D. Grady, T. Michaels, and R. Mitchell, Rev. Sci. Instrum. **41**, 984 (1970).

⁹L. M. Barker and R. E. Hollenbach, J. Appl. Phys. **41**, 4208 (1970).

¹⁰C. S. Yoo and Y. M. Gupta, J. Phys. Chem. **94**, 2857 (1990).

¹¹J. M. Winey and Y. M. Gupta, J. Phys. Chem. A **101**, 9333 (1997).

¹²G. Yu, G. Wang, H. Ishikawa, M. Umeno, T. Soga, T. Egawa, J. Watanabe, and T. Jimbo, Appl. Phys. Lett. **70**, 3209 (1997).

¹³V. S. Vavilov, Sov. Phys. Usp. **4**, 761 (1962); L. V. Keldysh, Sov. Phys. JETP **7**, 788 (1958); W. Franz, Z. Naturforsch. A **13**, 484 (1958).

¹⁴F. Bernardini, V. Fiorentini, and D. Vanderbilt, Phys. Rev. B **56**, R10024 (1997).

¹⁵J. Neugebauer and C. G. Van de Walle, Phys. Rev. B **50**, 8067 (1994).

¹⁶C. G. Van de Walle and J. Neugebauer, Appl. Phys. Lett. **70**, 2577 (1997).

¹⁷G. L. Bir and G. E. Pikus, *Symmetry and Strain Induced Effects in Semiconductors* (Wiley, New York, 1974).

¹⁸A. Shikanai, T. Azuhata, T. Sota, S. Chichibu, A. Kuramata, K. Horino, and S. Nakamura, J. Appl. Phys. **81**, 417 (1997).

¹⁹A. Polian, M. Grimsditch, and I. Grzegory, J. Appl. Phys. **79**, 3343 (1996).

²⁰P. Rigg and Y. M. Gupta, Phys. Rev. B **63**, 094112 (2001).